Pre-to-Post Operative MRI Generation with Retrieval-based Visual In-Context Learning

Bogyeong Kang[1], Sang-Jun Park[1], Minjoo Lim[1], Myeongkyun Kang[2], Keun-Soo Heo[1], Ji-Hye Oh[1], Hyun Jung Lee[1], and Tae-Eui Kam[1⋆]

[1] Department of Artificial Intelligence, Korea University, Seoul, South Korea.
{kangbk, kamte}@korea.ac.kr
[2] Department of Robotics and Mechatronics Engineering, Daegu Gyeongbuk Institute of Science and Technology (DGIST), Daegu, South Korea.

Abstract. Glioblastoma is an aggressive brain tumor requiring precise treatment planning. Magnetic resonance imaging (MRI) is essential for pre-operative assessment, surgical resection planning, and post-operative monitoring. Therefore, generating post-operative MRI from pre-operative MRI can assist neurosurgeons in many ways, such as predicting surgical outcomes and guiding treatment planning. However, generating post-operative MRI from pre-operative MRI is challenging, as the resection extent depends on tumor location and infiltration to minimize potential complications, necessitating consideration of surgical outcomes based on tumor location and shape. Furthermore, post-operative MRI differs significantly from pre-operative MRI due to structural and visual changes, such as tissue shift, edema, hemorrhage, and the resection region. To address these challenges, we propose a novel post-operative MRI generation method that generates post-operative MRI from pre-operative MRI using tumor-aware visual in-context learning. Specifically, we provide explicit visual instruction for generating post-operative MRI from pre-operative MRI, improving the capture of structural changes. To consider tumor-specific post-operative outcomes, we propose tumor-guided retrieval, which retrieves the tumor case most similar to the query pre-operative MRI, and a tumor-aware prompt adapter that integrates tumor resection and anatomical structure information. Our proposed method achieves superior performance on publicly available dataset and is the first to generate post-operative MRI from pre-operative MRI, introducing a new approach to improving patient prognosis.

Keywords: Post-operative MRI · MRI Generation · Diffusion Model

1 Introduction

Glioblastoma is a rapidly infiltrative brain tumor with a poor prognosis, necessitating accurate diagnosis for treatment planning and improving patient outcomes [2, 16, 19]. Magnetic resonance imaging (MRI) is essential for assessing

⋆ Corresponding author

glioblastoma, providing critical information for pre-operative diagnosis, post-operative monitoring, and treatment planning [6, 8, 18, 25]. Neurosurgeons determine the extent of surgical resection by analyzing past cases of pre- and post-operative MRI [27]. Generating post-operative MRI from pre-operative MRI allows neurosurgeons to estimate potential outcomes before surgery, significantly improving surgical and treatment planning.

Recent advances in generative models [10, 12, 23] have led to extensive research on image translation methods [13, 22, 32], which have primarily focused on preserving the structure of the source image while reflecting the style of the target image [13, 22, 32]. However, generating post-operative MRI from pre-operative MRI is far more challenging than previous methods [13, 22, 32] that focus only on style translation due to two challenges. First, post-operative MRI generation should consider post-operative outcomes specific to tumor location and shape [9, 11], as determining the extent of resection is crucial for minimizing patient complications when a tumor is located in a critical brain region or has diffusely infiltrated surrounding tissues [4, 11, 26]. Second, post-operative MRI generation should capture the visual and structural changes resulting from resection, as post-operative MRI exhibits differences compared to pre-operative MRI, including the resection region, brain tissue shift, edema, and hemorrhage [7, 20].

To address these challenges, we propose a novel post-operative MRI generation method that generates post-operative MRI from pre-operative MRI using tumor-aware visual in-context learning, enhancing the capture of structural changes and accurately reflecting the tumor resection region based on tumor location and shape. We provide explicit visual instruction for generating post-operative MRI from pre-operative MRI through **visual in-context learning**, improving the capture of structural changes between paired pre- and post-operative MRI and enhancing generation quality. To consider tumor-specific post-operative outcomes, we introduce **tumor-guided retrieval**, which retrieves an instruction pre- and post-operative MRI pair from another subject with a tumor location and shape closely matching those in the query pre-operative MRI. This approach provides instruction on information from similar tumor cases during post-operative MRI generation, allowing the capture of structural changes and tumor-specific resection outcomes to enhance the accuracy of post-operative MRI generation. Furthermore, we introduce a **tumor-aware prompt adapter** designed to capture not only the tumor location and anatomical structure in the pre-operative MRI but also the tumor resection region in the post-operative MRI, allowing the generated post-operative MRI to better reflect tumor-specific surgical outcomes. We demonstrate its effectiveness by achieving outstanding performance in generating post-operative MRI from pre-operative MRI using a publicly available LUMIERE [28] dataset.

The main contributions of our method can be summarized as follows:

- To the best of our knowledge, this is the first approach to generate post-operative MRI from pre-operative MRI using visual in-context learning, capturing visual and structural changes resulting from surgical resection.

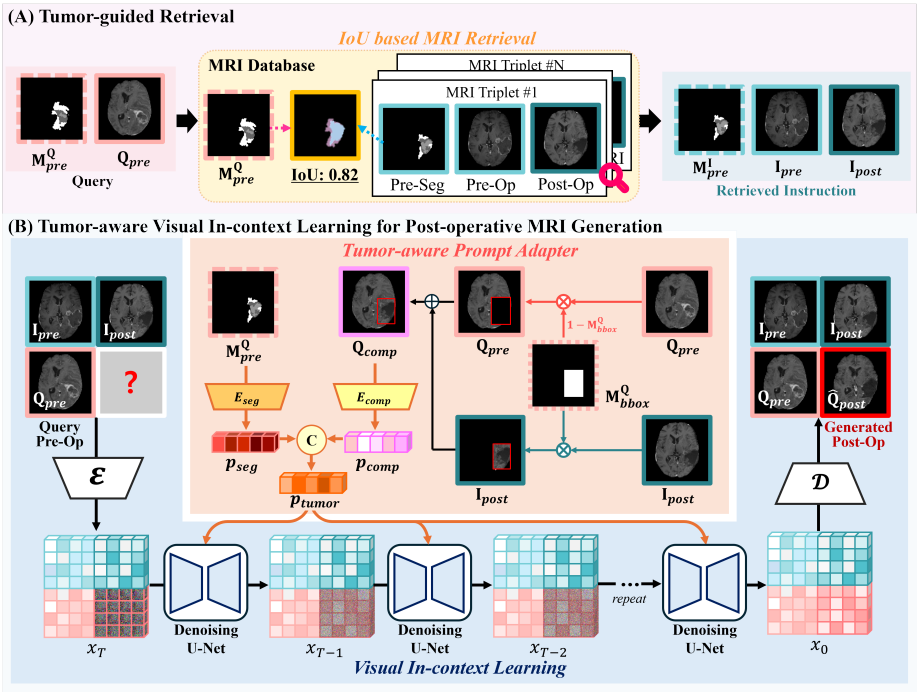

Fig. 1. Overview of the proposed method for post-operative MRI generation, which accurately reflects the tumor resection region and post-operative structural changes through two key components: (A) tumor-guided retrieval, (B) tumor-aware visual in-context learning for post-operative MRI generation.

– To consider tumor-specific post-operative outcomes, we propose tumor-guided retrieval, which retrieves pre- and post-operative MRI pairs with a tumor location and shape similar to the query, and a tumor-aware prompt adapter that integrates tumor resection and anatomical structure information.

2 Method

In this section, we describe our proposed method for post-operative MRI generation, which comprises two key components: (A) tumor-guided retrieval and (B) tumor-aware visual in-context learning for post-operative MRI generation. First, we retrieve MRI scans that closely match the tumor location and shape of the query pre-operative MRI to consider tumor-specific post-operative changes through tumor-guided retrieval. Then, we generate post-operative MRI with a tumor-aware prompt adapter and visual in-context learning to better capture tumor-specific structural changes resulting from resection.

2.1 Tumor-guided Retrieval

To consider tumor-specific post-operative outcomes, we design a tumor-guided retrieval strategy that retrieves a pre- and post-operative MRI pair with tumor location and shape closely matching those in the query pre-operative MRI. We construct an MRI database consisting of triplets: {Pre-operative MRI, Post-operative MRI, Pre-operative Segmentation Mask}, derived from the training dataset. Given the query pre-operative MRI Q_{pre} and its corresponding segmentation mask $\mathrm{M}^{\mathrm{Q}}_{pre}$, we compute the Intersection over Union (IoU) between the segmentation mask of the query pre-operative MRI and those of all triplets stored in the MRI database. We retrieve the MRI triplet with the highest IoU to ensure that the segmentation map includes a tumor region that best matches the location and shape of the tumor in the query pre-operative MRI. To provide more robust guidance, we select the top-k most similar triplets to be utilized as instructions for post-operative MRI generation, denoted as Instruction = $\{\mathrm{I}_{pre}$, I_{post}, $\mathrm{M}^{\mathrm{I}}_{pre}\}$, where I_{pre} and I_{post} are the retrieved pre- and post-operative MRI, and $\mathrm{M}^{\mathrm{I}}_{pre}$ is the corresponding segmentation mask. To further refine the precision of tumor-guided retrieval, we incorporate axial plane alignment in addition to segmentation mask similarity. Specifically, we restrict retrieval to MRI triplets whose axial plane range aligns with that of the query pre-operative scan, ensuring that retrieved images reflect tumors located within a similar axial plane.

2.2 Tumor-aware Visual In-context Learning for Post-operative MRI Generation

Tumor-aware Prompt Adapter. We design a tumor-aware prompt adapter that guides the generation of tumor-specific post-operative MRI by integrating information from the tumor resection region in the retrieved post-operative MRI and the anatomical structure in the pre-operative MRI. Given a retrieved instruction's post-operative MRI I_{post}, we integrate its tumor resection region with the anatomical structure of the query pre-operative MRI Q_{pre}. This is achieved through a compositing operation, which is formulated as follows: $\mathrm{Q}_{comp} = \mathrm{M}^{\mathrm{Q}}_{bbox} \cdot \mathrm{I}_{post} + (1 - \mathrm{M}^{\mathrm{Q}}_{bbox}) \cdot \mathrm{Q}_{pre}$, where Q_{pre} is the query pre-operative MRI, I_{post} is the post-operative MRI from the retrieved instruction, and $\mathrm{M}^{\mathrm{Q}}_{bbox}$ refers to the bounding box mask, which is derived from the segmentation mask of the query pre-operative MRI. Next, the composite image Q_{comp} is fed into E_{comp}, which consists of a pretrained image encoder of MedSAM [17] followed by multiple convolution and pooling layers. The Q_{comp} is processed by the pretrained image encoder to extract features, which are then passed through the subsequent layers and reshaped into a 1024-dimensional latent representation p_{comp}. Additionally, the pre-operative segmentation mask $\mathrm{M}^{\mathrm{Q}}_{pre}$ is fed into E_{seg}, where features are extracted using a convolutional layer, reshaped, and projected through a fully connected layer into a 1024-dimensional latent representation p_{seg}. Finally, the p_{seg} is then concatenated with the p_{comp} to form the final prompt embedding p_{tumor}. The p_{tumor} is injected into the Stable Diffusion [24] process through

cross-attention to guide tumor resection characteristics in the post-operative MRI and tumor location with anatomical structure in the pre-operative MRI.

Visual In-context Learning. To capture the structural changes between pre- and post-operative MRI, we generate the post-operative MRI $\hat{\mathrm{Q}}_{post}$ by adopting visual in-context learning [1, 31, 29]. In our visual in-context learning, we explicitly consider tumor-specific post-operative changes using the query pre-operative MRI Q_{pre} and the retrieved instruction pair $\{\mathrm{I}_{pre}, \mathrm{I}_{post}\}$ obtained by tumor-guided retrieval. To achieve this, we construct a grid-like image $Grid(\{\mathrm{I}_{pre}, \mathrm{I}_{post}, \mathrm{Q}_{pre}, B\})$. Here, B represents a blank image, which is reconstructed into $\hat{\mathrm{Q}}_{post}$ through the diffusion process. We employ the Stable Diffusion [24] that operates in the latent space rather than the pixel space. First, the grid-like image $Grid(\{\mathrm{I}_{pre}, \mathrm{I}_{post}, \mathrm{Q}_{pre}, B\})$ is encoded into a latent representation x_0 using a variational autoencoder [15]. During the forward process, noise is gradually added only to B region over time steps t, generating noisy representations x_t based on a noise scheduler [12]. In the reverse process, a denoising network iteratively removes noise from B through a Markov process [12], ultimately reconstructing x_0, which corresponds to the generated post-operative MRI $\hat{\mathrm{Q}}_{post}$. This process is formulated as $p_\theta(x_{t-1}|x_t, c)$ where θ represents the learnable parameters of the diffusion model, and c is the conditioning input [24]. In our task, c is the prompt p_{tumor} from the tumor-aware prompt adapter. The training objective of the diffusion model is to predict the added noise ϵ, and the loss function is formulated as follows [24]: $L_{LDM} = \mathbb{E}_{x_0,\epsilon,t}\left[\|\epsilon - \epsilon_\theta(x_t, t, c)\|^2\right]$, where ϵ_θ is the noise prediction network [24]. We adopt Classifier-Free Guidance [23], which enables the model to generate post-operative MRI by conditioning on retrieved instructions while maintaining flexibility in sampling.

3 Experiments and Results

3.1 Experiments Settings

Dataset and Implementation Details. We utilize the publicly available LUMIERE [28] dataset, containing 71 paired pre- and post-operative MRI scans, normalized to MNI space. Contrast-enhanced T1-weighted MRI is converted into 2D axial slices, from which tumor-containing slices with segmentation masks are selected. The dataset is split into 2,530 training and 205 testing slices. We train a Stable Diffusion [24] using AdamW [14] with a learning rate of 1e-5 and a cosine scheduler. We utilize the MedSAM [17] as an image encoder to extract features from the composite image and tumor-guided retrieval uses top-$k = 15$ for training and 1 for inference. During training, we randomly select one triplet from the retrieved top-15 triplets in each batch and use it as the instruction.

Competing Methods. We compare our performance against established diffusion based image editing methods [3, 12, 21, 30, 31] using SSIM, MS-SSIM,

Table 1. Comparison of post-operative MRI generation results with state-of-the-art image editing methods.

Method	SSIM (↑)	MS-SSIM (↑)	PSNR (↑)	LPIPS (↓)
DDPM [12]	0.5744	0.7587	31.23	0.1878
PBE [30]	0.6695	0.7295	31.09	0.1994
InstructPix2Pix [3]	0.6649	0.7594	31.53	0.1925
VISII [21]	0.6682	0.7611	31.50	0.1921
ImageBrush [31]	0.6718	0.7569	31.56	0.1928
Ours	**0.7001**	**0.7814**	**31.67**	**0.1845**

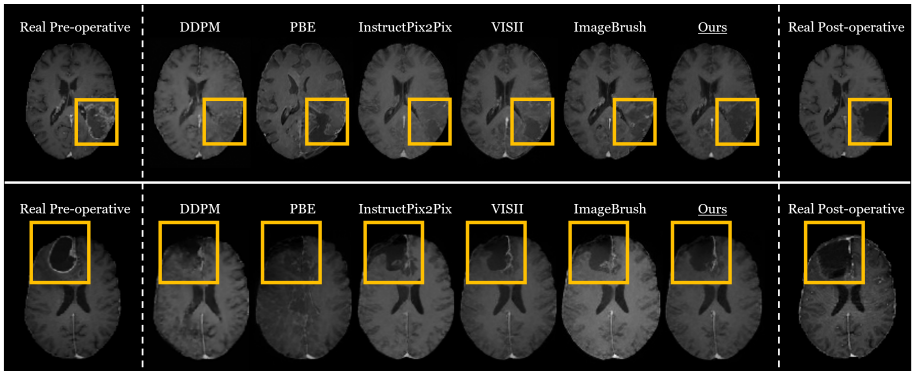

Fig. 2. Qualitative comparison of post-operative MRI generation with state-of-the-art image editing methods.

PSNR, and LPIPS as metrics. We train DDPM [12] by concatenating pre- and post-operative MRI. For PBE [30], we randomly select resection regions from post-operative MRI in the training dataset as exemplar images. For InstructPix2Pix [3] and VISII [21], we follow the same concatenation approach as DDPM and provide the text instruction "Post-operative glioblastoma MRI". For ImageBrush [31], we provide random instruction during visual in-context learning.

3.2 Main Results

To evaluate our approach for post-operative MRI generation, we conduct a comparative study on image editing methods [3, 12, 21, 30, 31]. Table 1 shows the performance results of post-operative MRI generation. Our method outperforms all image editing methods [3, 12, 21, 30, 31] across all evaluation metrics, achieving SSIM of 0.7001, MS-SSIM of 0.7814, PSNR of 31.67, and LPIPS of 0.1845. These results demonstrate that our approach is specifically tailored for generating post-operative MRI, effectively capturing tumor-specific post-operative changes. Furthermore, Fig. 2 presents the qualitative results of post-operative MRI generation from pre-operative MRI. Our method generates images that are the most similar to real post-operative MRI among all image editing methods [3,

Table 2. An ablation study on different retrieval strategies and the effectiveness of the two prompts in our tumor-aware prompt adapter. We evaluate three retrieval strategies: Random (random selection), Image-retrieval (retrieval based on cosine similarity in the image embedding space), and Ours (tumor-guided retrieval). Additionally, we assess the impact of two prompts: p_{seg} (segmentation mask of the input pre-operative MRI) and p_{comp} (composite image).

Method	SSIM (↑)	MS-SSIM (↑)	PSNR (↑)	LPIPS (↓)
Random	0.6823	0.7654	31.59	0.1875
Image-retrieval	0.6846	0.7684	31.63	0.1869
Ours ($w/o.$ p_{seg})	0.6835	0.7703	31.60	0.1887
Ours ($w/o.$ p_{comp})	0.6784	0.7758	31.61	0.1863
Ours	**0.7001**	**0.7814**	**31.67**	**0.1845**

12, 21, 30, 31]. In particular, as shown in Fig. 2, DDPM [12], PBE [30], InstructPix2Pix [3], and VISII [21] fail to reflect the post-operative tumor resection region, often generating blurred and indistinct structures instead. These findings highlight the importance of visual in-context learning for capturing structural changes caused by resection in post-operative MRI generation. Compared to ImageBrush [31], which also employs visual in-context learning, our method demonstrates visibly superior performance. This improvement can be attributed to our tumor-guided retrieval strategy, which tailors instructions based on tumor location and shape. Additionally, our tumor-aware prompt adapter explicitly incorporates the pre-operative tumor location and post-operative resection region, enhancing the post-operative MRI generation. These results demonstrate that our approach effectively captures tumor-specific post-operative changes, enabling accurate generation of post-operative MRI.

3.3 Ablation Study

Effectiveness of tumor-guided retrieval. We conduct an ablation study by comparing post-operative MRI generation using random selection and image-retrieval instead of our tumor-guided retrieval. In our experiments, random selection refers to selecting an MRI instruction randomly from the training dataset. The image-retrieval strategy embeds images into latent space using a ViT encoder [5] and retrieves the top-k most similar images based on cosine similarity. As shown in Fig. 3, the random selection strategy selects the instruction that differ entirely in anatomical structure, as well as in tumor location and shape. The image-retrieval strategy selects the instruction with a similar overall anatomical structure but differing tumor location and shape. As shown in Table 2, Ours outperforms both random selection and image-retrieval, achieving the best performance. Notably, the image-retrieval strategy performs comparably to random selection, indicating its limited effectiveness for post-operative MRI generation. This limitation arises because the image-retrieval strategy primarily relies on overall anatomical similarity and does not consider the tumor location and shape. However, since the tumor region plays a critical role in post-operative MRI

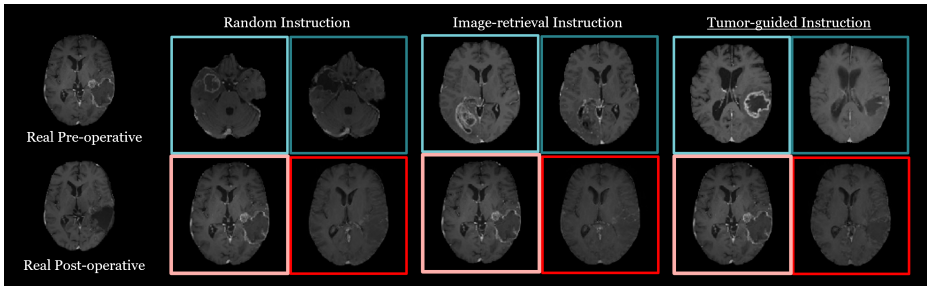

Fig. 3. Qualitative results from the ablation study comparing retrieval strategies for visual in-context learning in post-operative MRI generation.

generation, considering it in retrieval is essential for achieving promising performance. These findings emphasize the importance of tumor-guided retrieval, demonstrating that explicitly considering tumor-specific characteristics is crucial for accurate post-operative MRI generation.

Effectiveness of tumor-aware prompt adapter. We further conduct an ablation study to evaluate the effectiveness of our tumor-aware prompt adapter. Specifically, we evaluate the impact of different conditioning strategies in the Stable Diffusion process by modifying the injected information. First, we use only the composite image as the prompt, without the segmentation mask (Ours ($w/o.\ p_{seg}$)). As shown in Table 2, this approach results in lower performance compared to Ours, which utilizes both the composite image and the segmentation mask. This highlights the importance of leveraging the input pre-operative segmentation mask as a prompt, since it provides spatial guidance for the tumor's location and shape. Notably, using only the segmentation mask as the prompt, without the composite image (Ours ($w/o.\ p_{comp}$)), results in even more significant performance degradation. This suggests that the composite image serves as a critical prompt that reflects tumor-specific surgical outcomes. Therefore, these results demonstrate that our tumor-aware prompt adapter captures tumor-specific post-operative outcomes, enabling more accurate post-operative MRI generation.

4 Conclusion

We propose a novel method for post-operative MRI generation from pre-operative MRI. Our proposed method integrates tumor-guided retrieval, a tumor-aware prompt adapter, and visual in-context learning to better capture post-operative structural changes and accurately reflect tumor resection based on tumor location and shape. We demonstrate the superiority of our proposed method in generating post-operative MRI on the LUMIERE dataset, highlighting its potential for improving surgical planning and patient-specific treatment strategies.

Acknowledgments. This work was supported by Institute of Information & communications Technology Planning & Evaluation (IITP) grant funded by the Korea government (MSIT) (No. RS-2019-II190079, Artificial Intelligence Graduate School Program(Korea University)), the National Research Foundation of Korea (NRF) grant funded by the Korea government (MSIT) (No. RS-2023-00212498), the Institute of Information & communications Technology Planning & Evaluation (IITP) grant funded by the Korea government (MSIT) (RS-2024-00457882, Artificial Intelligence Research Hub Project), and the MSIT (Ministry of Science and ICT), Korea, under the ITRC (Information Technology Research Center) support program (IITP-2025-RS-2024-00436857) supervised by the IITP (Institute for Information & Communications Technology Planning & Evaluation).

Disclosure of Interests. The authors have no competing interests to declare that are relevant to the content of this article.

References

1. Bar, A., Gandelsman, Y., Darrell, T., Globerson, A., Efros, A.: Visual prompting via image inpainting. Advances in Neural Information Processing Systems **35**, 25005–25017 (2022)
2. Booth, T.C., Luis, A., Brazil, L., Thompson, G., Daniel, R.A., Shuaib, H., Ashkan, K., Pandey, A.: Glioblastoma post-operative imaging in neuro-oncology: current UK practice (gin cup study). European Radiology **31**, 2933–2943 (2021)
3. Brooks, T., Holynski, A., Efros, A.A.: Instructpix2pix: Learning to follow image editing instructions. In: Proceedings of the IEEE/CVF Conference on Computer Vision and Pattern Recognition. pp. 18392–18402 (2023)
4. Brown, T.J., Brennan, M.C., Li, M., Church, E.W., Brandmeir, N.J., Rakszawski, K.L., Patel, A.S., Rizk, E.B., Suki, D., Sawaya, R., et al.: Association of the extent of resection with survival in glioblastoma: a systematic review and meta-analysis. JAMA oncology **2**(11), 1460–1469 (2016)
5. Dosovitskiy, A.: An image is worth 16x16 words: Transformers for image recognition at scale. arXiv preprint arXiv:2010.11929 (2020)
6. Farace, P., Amelio, D., Ricciardi, G.K., Zoccatelli, G., Magon, S., Pizzini, F., Alessandrini, F., Sbarbati, A., Amichetti, M., Beltramello, A.: Early MRI changes in glioblastoma in the period between surgery and adjuvant therapy. Journal of Neuro-oncology **111**, 177–185 (2013)
7. Farace, P., Giri, M., Meliado, G., Amelio, D., Widesott, L., Ricciardi, G.K., Dall'Oglio, S., Rizzotti, A., Sbarbati, A., Beltramello, A., et al.: Clinical target volume delineation in glioblastomas: pre-operative versus post-operative/pre-radiotherapy mri. The British journal of radiology **84**(999), 271–278 (2011)
8. Garcia-Ruiz, A., Naval-Baudin, P., Ligero, M., Pons-Escoda, A., Bruna, J., Plans, G., Calvo, N., Cos, M., Majos, C., Perez-Lopez, R.: Precise enhancement quantification in post-operative MRI as an indicator of residual tumor impact is associated with survival in patients with glioblastoma. Scientific Reports **11**(1), 695 (2021)
9. Gerritsen, J.K.W., Young, J.S., Krieg, S.M., Jungk, C., Ille, S., Schucht, P., Nahed, B.V., Broekman, M.L.D., Berger, M., De Vleeschouwer, S., et al.: Resection versus

biopsy in patients with glioblastoma (resbiop study): study protocol for an international multicentre prospective cohort study (encram 2202). BMJ Open **14**(9) (2024)
10. Goodfellow, I., Pouget-Abadie, J., Mirza, M., Xu, B., Warde-Farley, D., Ozair, S., Courville, A., Bengio, Y.: Generative adversarial nets. Advances in Neural Information Processing Systems **27** (2014)
11. de Haan, Y., Moussa, A., Gerritsen, J., Schnitzler, S., Dirven, C., Vincent, A.: P27. 03. b biopsy versus resection in glioblastoma treatment: A propensity score-matched analysis of a retrospective cohort. Neuro-Oncology **26**, 136–137 (2024)
12. Ho, J., Jain, A., Abbeel, P.: Denoising diffusion probabilistic models. Advances in Neural Information Processing Systems **33**, 6840–6851 (2020)
13. Kang, B., Nam, H., Kang, M., Heo, K.S., Lim, M., Oh, J.H., Kam, T.E.: Target-aware cross-modality unsupervised domain adaptation for vestibular schwannoma and cochlea segmentation. Scientific Reports **14**(1), 27883 (2024)
14. Kingma, D.P.: Adam: A method for stochastic optimization. arXiv preprint arXiv:1412.6980 (2014)
15. Kingma, D.P., Welling, M., et al.: Auto-encoding variational bayes (2013)
16. Kubben, P.L., ter Meulen, K.J., Schijns, O.E., ter Laak-Poort, M.P., van Overbeeke, J.J., van Santbrink, H.: Intraoperative MRI-guided resection of glioblastoma multiforme: a systematic review. The Lancet Oncology **12**(11), 1062–1070 (2011)
17. Ma, J., He, Y., Li, F., Han, L., You, C., Wang, B.: Segment anything in medical images. Nature Communications **15**(1), 654 (2024)
18. Majós, C., Cos, M., Castañer, S., Gil, M., Plans, G., Lucas, A., Bruna, J., Aguilera, C.: Early post-operative magnetic resonance imaging in glioblastoma: correlation among radiological findings and overall survival in 60 patients. European Radiology **26**, 1048–1055 (2016)
19. McGirt, M.J., Villavicencio, A.T., Bulsara, K.R., Friedman, A.H.: MRI-guided stereotactic biopsy in the diagnosis of glioma: comparison of biopsy and surgical resection specimen. Surgical Neurology **59**(4), 279–283 (2003)
20. Miao, X., Chen, H., Tang, M., Huang, D., Gao, T., Chen, Y.: Post-operative MRI synthesis from pre-operative MRI and post-operative CT using conditional GAN for the assessment of degree of resection. Displays **83**, 102742 (2024)
21. Nguyen, T., Li, Y., Ojha, U., Lee, Y.J.: Visual instruction inversion: Image editing via image prompting. Advances in Neural Information Processing Systems **36**, 9598–9613 (2023)
22. Park, T., Efros, A.A., Zhang, R., Zhu, J.Y.: Contrastive learning for unpaired image-to-image translation. In: European Conference on Computer Vision. pp. 319–345. Springer (2020)
23. Ramesh, A., Dhariwal, P., Nichol, A., Chu, C., Chen, M.: Hierarchical text-conditional image generation with clip latents. arXiv preprint arXiv:2204.06125 **1**(2), 3 (2022)
24. Rombach, R., Blattmann, A., Lorenz, D., Esser, P., Ommer, B.: High-resolution image synthesis with latent diffusion models. In: Proceedings of the IEEE/CVF Conference on Computer Vision and Pattern Recognition. pp. 10684–10695 (2022)
25. Rykkje, A.M., Larsen, V.A., Skjøth-Rasmussen, J., Nielsen, M.B., Carlsen, J.F., Hansen, A.E.: Timing of early postoperative MRI following primary glioblastoma surgery—a retrospective study of contrast enhancements in 311 patients. Diagnostics **13**(4), 795 (2023)
26. Sanai, N., Berger, M.S.: Glioma extent of resection and its impact on patient outcome. Neurosurgery **62**(4), 753–766 (2008)

27. Shukla, G., Alexander, G.S., Bakas, S., Nikam, R., Talekar, K., Palmer, J.D., Shi, W.: Advanced magnetic resonance imaging in glioblastoma: a review. Chinese Clinical Oncology **6**(4), 40–40 (2017)
28. Suter, Y., Knecht, U., Valenzuela, W., Notter, M., Hewer, E., Schucht, P., Wiest, R., Reyes, M.: The LUMIERE dataset: Longitudinal glioblastoma MRI with expert RANO evaluation. Scientific Data **9**(1), 768 (2022)
29. Wang, X., Wang, W., Cao, Y., Shen, C., Huang, T.: Images speak in images: A generalist painter for in-context visual learning. In: Proceedings of the IEEE/CVF Conference on Computer Vision and Pattern Recognition. pp. 6830–6839 (2023)
30. Yang, B., Gu, S., Zhang, B., Zhang, T., Chen, X., Sun, X., Chen, D., Wen, F.: Paint by example: Exemplar-based image editing with diffusion models. In: Proceedings of the IEEE/CVF Conference on Computer Vision and Pattern Recognition. pp. 18381–18391 (2023)
31. Yang, Y., Peng, H., Shen, Y., Yang, Y., Hu, H., Qiu, L., Koike, H., et al.: Imagebrush: Learning visual in-context instructions for exemplar-based image manipulation. Advances in Neural Information Processing Systems **36**, 48723–48743 (2023)
32. Zhu, J.Y., Park, T., Isola, P., Efros, A.A.: Unpaired image-to-image translation using cycle-consistent adversarial networks. In: Proceedings of the IEEE International Conference on Computer Vision. pp. 2223–2232 (2017)